ADVANCED FUNCTIONAL MATERIALS
www.afm-journal.de

Materials Views
www.MaterialsViews.com

# Increased Work Function in Few-Layer Graphene Sheets via Metal Chloride Doping

*Ki Chang Kwon, Kyoung Soon Choi, and Soo Young Kim**

**A chemical approach to controlling the work function of few-layer graphene is investigated. Graphene films are synthesized on Cu foil by chemical vapor deposition. Six metal chlorides, $AuCl_3$, $IrCl_3$, $MoCl_3$, $OsCl_3$, $PdCl_2$, and $RhCl_3$, are used as dopants. The sheet resistance of the doped graphene decreases from 1100 Ω/sq to ≈500–700 Ω/sq and its transmittance at 550 nm also decreases from 96.7% to 93% for 20 mM $AuCl_3$ due to the formation of metal particles. The sheet resistance and transmittance are reduced with increasing metal chloride concentration. The G peak in the Raman spectra is shifted to a higher wavenumber after metal chloride doping, which indicates a charge transfer from graphene to metal ions. The intensity ratio of $I_{C=C}/I_{C-C}$ increases with doping, indicating an electron transfer from graphene sheets to metal ions. Ultraviolet photoemission spectroscopy data shows that the work function of graphene increases from 4.2 eV to 5.0, 4.9, 4.8, 4.68, 5.0, and 5.14 eV for the graphene with 20 mM $AuCl_3$, $IrCl_3$, $MoCl_3$, $OsCl_3$, $PdCl_2$, and $RhCl_3$, respectively. It is considered that spontaneous charge transfer occurs from the specific energy level of graphene to the metal ions, thus increasing the work function.**

## 1. Introduction

Graphene, a single layer of $sp^2$-bonded carbon atoms, has attracted much attention due to its unique physical properties such as high mobility of charge carriers, anomalous quantum Hall effect, superior thermal/electrical conductivity, ballistic transport properties, and longest mean free path at room temperature.[1–6] The electronic properties of graphene sheets have recently attracted strong experimental and theoretical interest. Recently, large area graphene sheets were successfully synthesized by chemical vapor deposition (CVD).[7–9] One of the most attractive applications of large-scale graphene is as flexible transparent conducting films for electronic devices. For application to a large-area, flexible transparent conducting electrode, many researchers have focused on the synthesis of graphene with a high transmittance (>90%) and low sheet resistance (<200 Ω/sq.). The methods for achieving high transmittance and low sheet resistance with easy synthesis are reported to include control of individual grain and grain boundaries, non-catalytic CVD, low-temperature growth for easy synthesis, roll-to-roll production of graphene films.[10–13] Transmittance and sheet resistance have thereby become acceptable for replacing the commercial transparent conducting electrodes such as indium tin oxide (ITO). Even though graphene was reported to be used as a transparent electrode in light emitting diodes, organic light emitting diodes, and organic solar cells, graphene-based devices have usually underperformed relative to ITO-based ones.[14–20] One of these problems was induced by the energy level difference between the graphene electrode and the other active layers in electronic devices. Using a high work function metal as an anode and a low work function metal as a cathode is adequate to reduce the potential barrier. Therefore, modulation of the work function in the graphene layer is crucial for improving device performances. Attempts have been made to modulate the work function in graphene by controlling the electronic structure using an Au-ion, $NH_3$, self-assembled monolayer or metal oxide interlayer.[21–26] Chemical doping was reported to be effective for tailoring the electrical properties of graphene and modulating the work function of graphene by charge transfer on the graphene sheet.

Metals with high work function include Au, Ir, Mo, Os, Pd, and Rh whose values are 5.47, 5.67, 4.95, 5.93, 5.6, and 4.98 eV, respectively.[27] Metal chlorides can be added in these metals so that they are soluble in specific solvents, which makes simple process for doping. Furthermore, metal ions with positive charge ($Me^{x+}$) in metal chlorides are spontaneously reduced to metal ions with zero charge ($Me^0$) after taking electrons from other materials due to their negative Gibbs free energy. Therefore, the use of $AuCl_3$, $IrCl_3$, $MoCl_3$, $OsCl_3$, $PdCl_3$, and $RhCl_3$ as dopants on graphene is expected to increase its work function. Furthermore, such adsorption-induced chemical doping adjusts the Fermi level without introducing substitutional impurities, or basal plane reactions, that interrupt the conjugated network.

In the present work, we investigated the increased work function in the graphene layer achieved by chemical doping using six metal chlorides as the p-dopant. $AuCl_3$, $IrCl_3$, $MoCl_3$, $OsCl_3$, $PdCl_2$, and $RhCl_3$ were used as p-dopant materials. The electrical properties of the metal-doped graphene were measured by 4-point probe. The optical properties of the metal-doped graphene layer were characterized with UV-visible spectra and optical microscopy (OM). X-ray photoemission spectroscopy

K. C. Kwon, K. S. Choi, Prof. S. Y. Kim
School of Chemical Engineering and Materials Science
Chung Ang University
Seoul, Republic of Korea
E-mail: sooyoungkim@cau.ac.kr

DOI: 10.1002/adfm.201200997

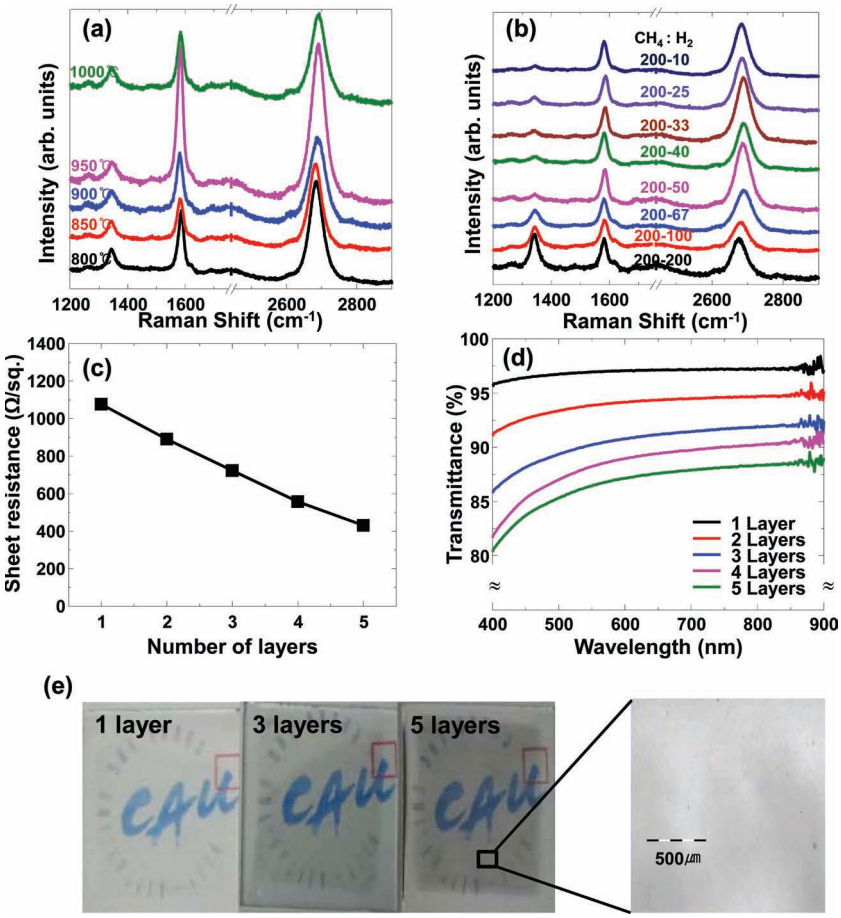


**Figure 1.** a) Change of Raman spectra as a function of growth temperature. The gas ratio of $CH_4$ to $H_2$ was fixed at 6:1. b) Change of Raman spectra as a function of gas ratio. The synthesis temperature was fixed at 950 °C. c) Change of sheet resistance as a function of the number of graphene layers. d) Change of transmittance as a function of the number of graphene layers. e) Photographic images of 1-, 3-, and 5-layer graphene on glass substrate.

(XPS) and Raman spectroscopy were used to characterize the doping process. Scanning electron microscopy (SEM) and energy dispersive spectroscopy (EDS) were used to examine the surface of the p-doped graphene layer. The change of work function after metal doping was confirmed by ultraviolet photoemission spectroscopy (UPS). The data of sheet resistance, Raman spectra, XPS, and UPS were obtained from same graphene film doped with each metal chloride at a concentration of 20 mM. Based on these measurements, the effect of the six metal chlorides on the change of work function in graphene sheets is discussed.

## 2. Results and Discussion

### 2.1. Optimization of Graphene Synthesis Condition

**Figure 1**a shows the change of Raman spectra as a function of growth temperature. The gas ratio of $CH_4$ to $H_2$ was fixed at 6:1. The G peak around 1550 $cm^{-1}$ was due to the in-plane bond-stretching motion of the $sp^2$-bonded carbon atoms and the 2D peak around 2700 $cm^{-1}$ to the monolayer graphene. The D peak around 1360 $cm^{-1}$ is absent in perfect graphite and indicates the presence of disorder.[8] No peak shift occurred as the growth temperature was increased. The intensity ratio of G peak to D peak ($I_G/I_D$) increased from 2.21 to 6.43 and that of 2D peak to G peak ($I_{2D}/I_G$) decreased from 2.10 to 1.13 as the temperature was increased from 850 °C to 950 °C. The intensity ratio data are summarized in **Table 1**. Because the D peak indicates the presence of defects, 950 °C was selected as the growth temperature due to the highest $I_G/I_D$. To determine the best $CH_4$ to $H_2$ gas ratio at 950 °C, the change of Raman spectra was investigated as a function of gas ratio, as shown in Figure 1b. The $I_G/I_D$ and $I_{2D}/I_G$ data are summarized in **Table 2**. A $CH_4$: $H_2$ ratio of 6:1 was the best growth condition due to the highest values of $I_G/I_D$ and $I_{2D}/I_G$. Figure 1c,d show the change of sheet resistance and transmittance according to the number of graphene layers. The sheet resistance of monolayer graphene was 1.1 kΩ/sq. and the transmittance at 550 nm was 97%. Both the transmittance and sheet resistance of the graphene film decreased with increasing number of layers. The sheet resistance of 5-layer graphene with was 450 Ω/sq. and the transmittance at 550 nm was 87%. The photographic images of 1-, 3-, and 5-layer graphene on glass substrate are shown in Figure 1e. The OM image of graphene shown in Figure 1e reveals a clean and continuous graphene surface.

### 2.2. Characteristics and Properties of P-Doped Graphene Film

Metal chloride solutions with different concentrations were spin-coated at 2500 rpm for 1 min with 300 μL on the transferred graphene substrate, as shown in **Figure 2**a. To investigate the effect of p-dopant on the graphene conductivity, the sheet resistance of pristine graphene (PG) and the doped graphene sheets was measured, as shown in Figure 2b. The

**Table 1.** Intensity ratio of $I_G/I_D$ and $I_{2D}/I_G$ as a function of growth temperature.

| Temperature [°C] | $I_G/I_D$ | $I_{2D}/I_G$ |
|---|---|---|
| 800 | 2.69 | 1.63 |
| 850 | 2.21 | 2.10 |
| 900 | 2.64 | 1.46 |
| 950 | 6.43 | 1.13 |
| 1000 | 2.60 | 1.49 |

**Table 2.** Intensity ratio of $I_G/I_D$ and $I_{2D}/I_G$ as a function of gas ratio.

| $CH_4$:$H_2$ | $I_G/I_D$ | $I_{2D}/I_G$ |
|---|---|---|
| 200:200 | 0.93 | 1.15 |
| 200:100 | 1.29 | 1.00 |
| 200:67 | 1.77 | 1.44 |
| 200:50 | 4.75 | 1.90 |
| 200:40 | 6.00 | 1.42 |
| 200:33 | 6.40 | 1.75 |
| 200:25 | 3.71 | 1.77 |
| 200:10 | 4.40 | 2.23 |

monolayer PG on glass substrates was exposed to 60 wt% $HNO_3$ in vapor phase. The sheet resistance of $HNO_3$-treated sample decreased from 1100 Ω/sq. to 750 Ω/sq. $HNO_3$ is known to be a p-dopant in graphitic materials, where an electron is transferred from the graphene to the $HNO_3$ as a charge-transfer complex is formed. Therefore, we considered that $HNO_3$ surface treatment increased the p-type properties of graphene, thus decreasing the sheet resistance. Metal chloride doping solution with a concentration of 20 mM was spin-coated on the $HNO_3$-doped samples. The averaged sheet resistance decreased from 750 Ω/sq. to 500, 600, 720, 700, 520, and 620 Ω/sq. with $AuCl_3$, $IrCl_3$, $MoCl_3$, $OsCl_3$, $PdCl_3$, and $RhCl_3$ dopants, respectively. The statistical data of sheet resistance for each metal chloride is presented in Figure SI1 (Supporting Information). $AuCl_3$-doped sample showed the lowest sheet resistance, and all samples exhibited lower resistance than that of $HNO_3$-doped graphene. The degree of change in sheet resistance as a function of p-dopants is depicted in the inset of Figure 2b. There is slight difference in sheet resistance of PG in each sample, as shown in Figure SI2 (Supporting Information). Therefore, the sheet resistance was normalized with respect to PG in order to avoid the ambiguity which comes from sample-to-sample variation. We considered that this significant drop in sheet resistance indicates the donation of electrons from graphene to the metal particles by reducing $Au^{3+}$, $Ir^{3+}$, $Mo^{3+}$, $Os^{3+}$, $Pd^{3+}$, and $Rh^{3+}$ to $Au^0$, $Ir^0$, $Mo^0$, $Os^0$, $Pd^0$, and $Rh^0$, respectively.

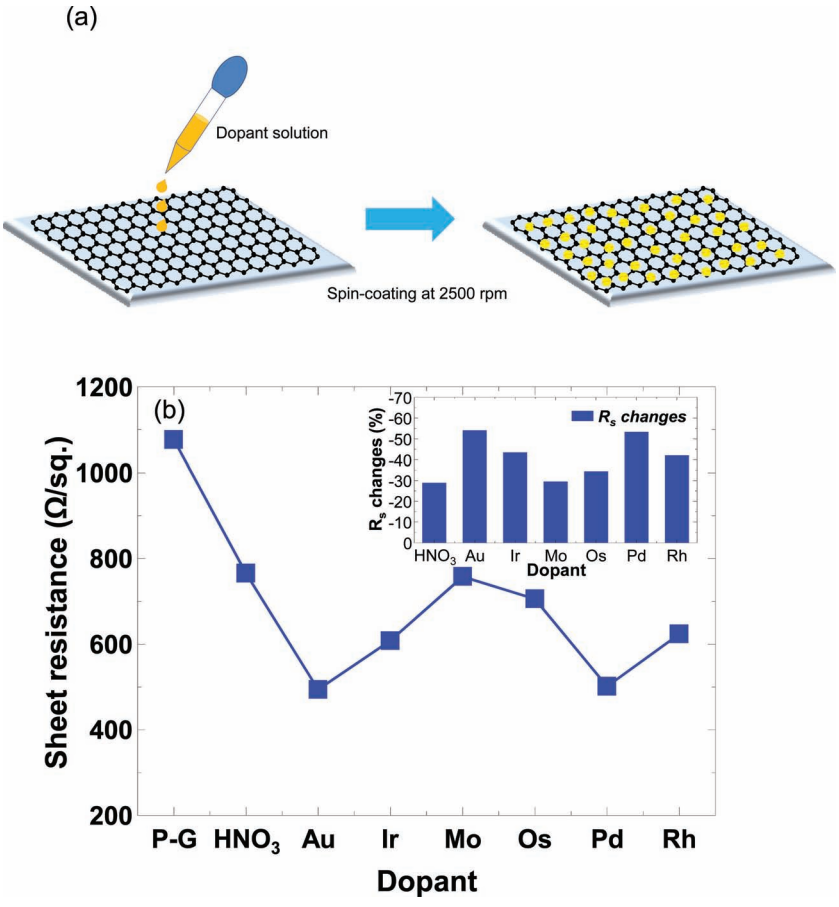


**Figure 2.** a) Schematic image of the doping process. Six metal chloride solutions with three different concentrations were spin-coated at 2500 rpm for 1 min with 300 µL on the transferred graphene substrate. b) Sheet resistance of PG and doped graphene sheets. The degree of change in the sheet resistance as a function of p-dopants is depicted in the inset of (b). The highest and lowest degrees of sheet resistance reduction were about 55% for $AuCl_3$ and about 32% for $MoCl_3$, respectively.

**Figure 3**a shows the transmittance of graphene films doped with 5 mM solution in the 400–900 nm wavelength range. The transmittance of PG at 550 nm was about 96.7%. However, the transmittance of p-doped graphene at 550 nm was decreased by between 94.5% for $AuCl_3$ and 86.2% for $MoCl_3$. Figure 3b shows the transmittance of graphene films doped with 20 mM solution. The transmittance of graphene films doped with 20 mM solution was lower than that with 5 mM solution. These results indicated that the sample transmittance was decreased with increasing doping solution concentration. OM images of the graphene films doped with 20 mM solution are shown in Figure 3c. Metal particles, thought to have been formed by the transfer of electrons from graphene to metal ions, were uniformly dispersed on the graphene surface. Therefore, the number of metal particles increased with increasing doping solution concentration, thus decreasing the transmittance of graphene.

**Figure 4**a displays the SEM image and EDS spectra of the graphene doped with 20 mM solution. Particles, which were absent on PG, were observed on the surface of p-doped graphene. The EDS spectra indicated that these metal particles originated from the doping solution. The positive charge of the metal ions in metal chlorides is reduced to zero after the capture of electrons from graphene, leading to the formation of metal particles on the graphene surface. Therefore, we considered that graphene was well doped with metal

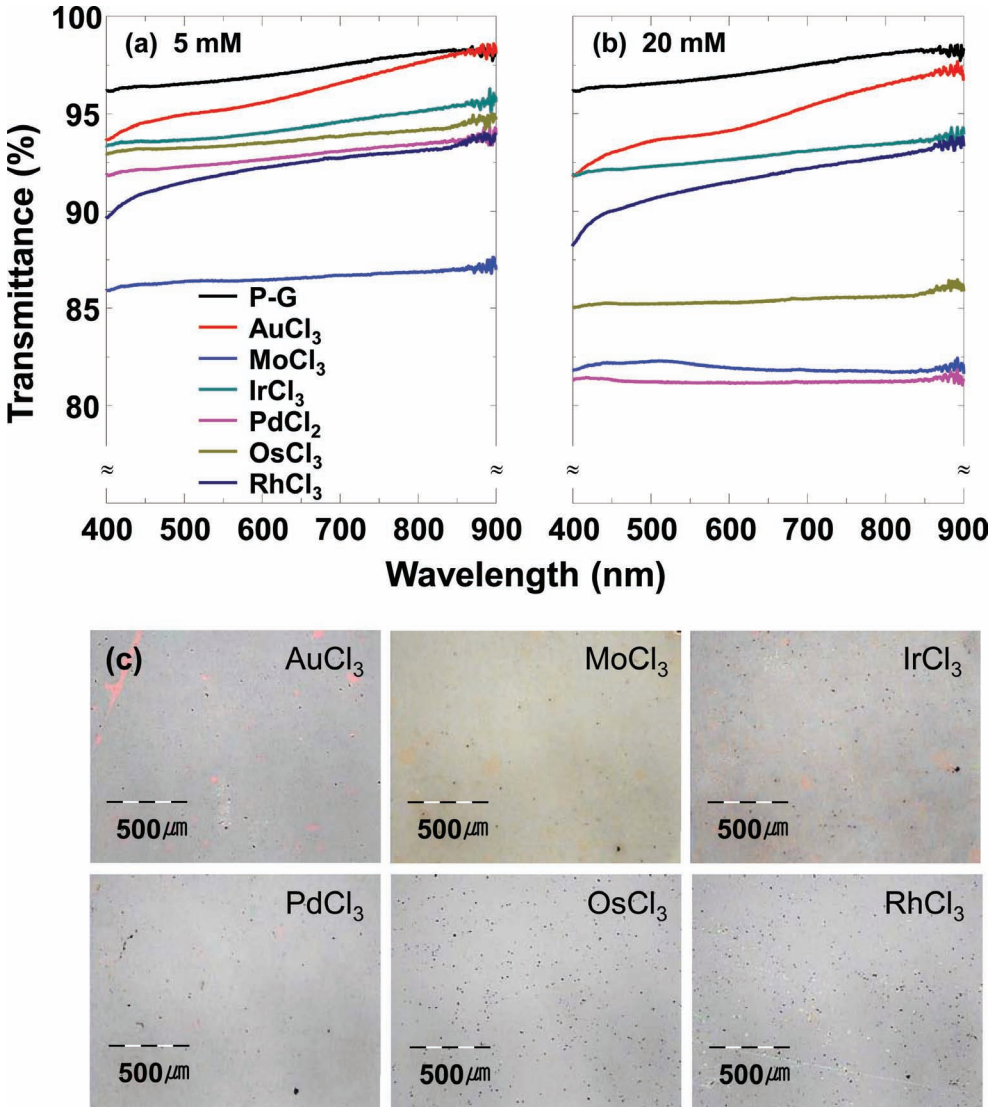


**Figure 3.** a) Transmittance data of PG and graphene sheets doped with six metal chlorides at a concentration of 5 mM. The transmittance of pristine graphene sheet at 550 nm was about 96.7%. The graphene doped with $MoCl_3$ at 550 nm showed the lowest transmittance of 86%. b) Transmittance data of PG and graphene sheets doped with six metal chlorides at a concentration of 20 mM. The graphene doped with $MoCl_3$ at 550 nm showed the lowest transmittance of 81%. c) OM images of the graphene doped with 20 mM solution. Metal particles can be seen uniformly dispersed on the graphene surface.

chloride solution. Figure 4b shows the Raman spectra of p-doped graphene with metal chloride solutions. The G band was shifted to a higher wavenumber of about 21.2, 12.5, 6.5, 5.4, 8.2, and 7.1 $cm^{-1}$ for $AuCl_3$, $IrCl_3$, $MoCl_3$, $OsCl_3$, $PdCl_3$, and $RhCl_3$ dopants, respectively. Both electrons and hole doping on graphene have been reported to shift the G band to a higher wavenumber.[28,29] Therefore, the large peak shift of the G band in graphene indicates the strongly doped state of graphene. In addition, there was no detectable shift of the D peak between doped graphene and PG, suggesting that the metal chloride doping process does not increase the number of defects in graphene. Therefore, it is considered that the chemical doping of graphene with metal chlorides is more effective than destructive doping techniques such as substitutional doping or covalent functionalization of graphene.

### 2.3. The Increased Work Function in p-Doped Graphene Film

**Figure 5**a shows the XPS C 1*s* spectra of the p-doped graphene film. In order to separate the chemical bonding states, including those in the spectra, the spectral line shape was simulated using a suitable combination of Gaussian and Lorentzian functions.[30] For all fitting multiplets, the full-width-at-half-maximums were fixed accordingly. The C 1*s* peak of PG was separated into four components: $sp^2$ carbon (C=C) at 284.3 eV,

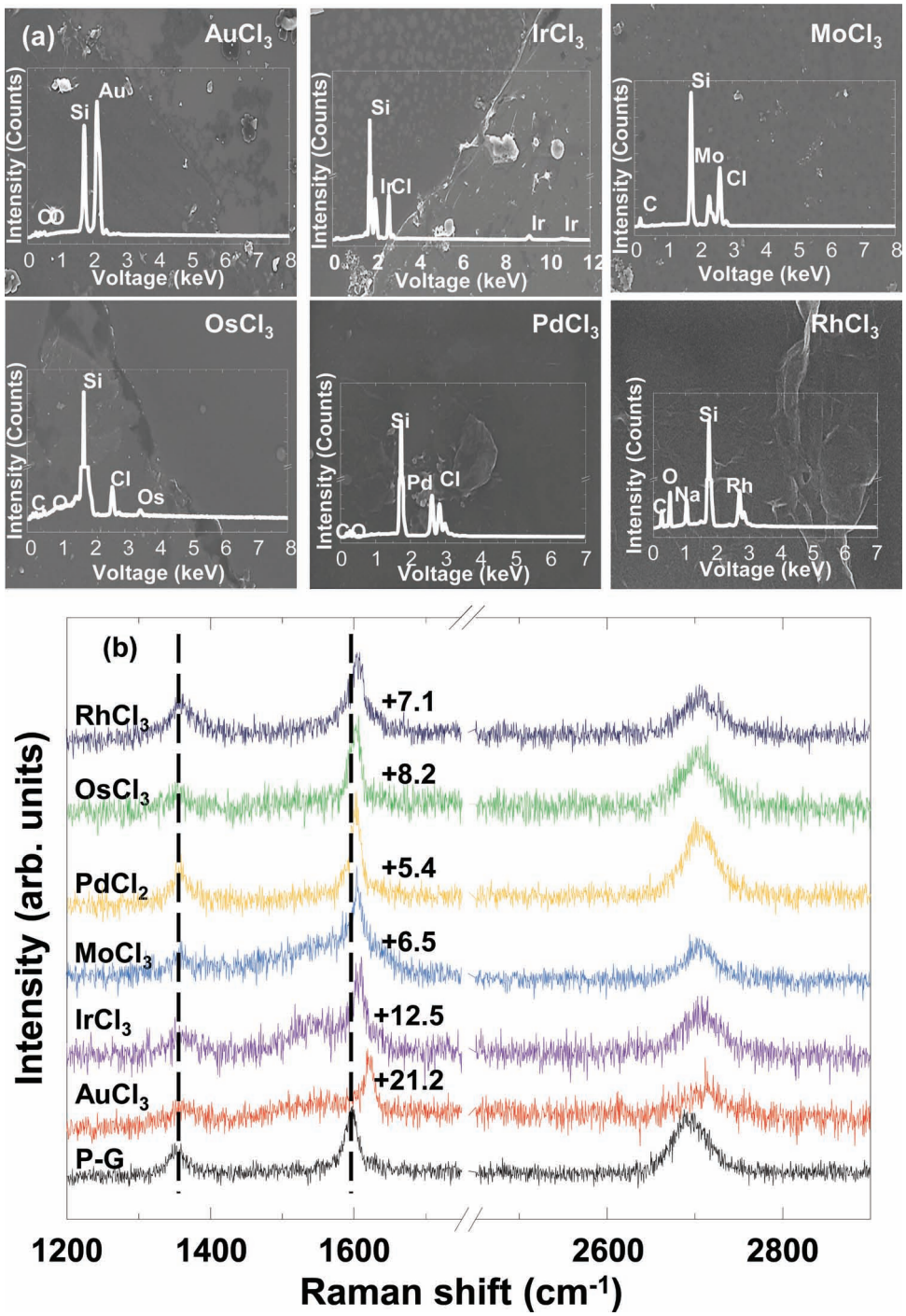


**Figure 4.** a) SEM image and EDS spectra of graphene doped with 20 mM solution. The evident metal particles, which were not observed in PG, originated from the doping solution. b) Raman spectra of p-doped graphene with six metal chloride solutions. The large peak shift of the G band in graphene indicates the strongly doped states of graphene.

$sp^3$ carbon (C−C) at 285.4 eV, C−O bond at 286.6 eV, and a carbonyl group (C=O) near 288.5 eV.[22] Although PG was synthesized by CVD, it had some oxide functional groups on its surface, which were thought to have been induced by the wet transfer process that used acetone, isopropyl alcohol, and de-ionized water. No peak shift was found in the C=C and C−C peaks. The peak intensity of the C−C ($I_{C-C}$) and C=O bonds was reduced, but that of the C=C bond ($I_{C=C}$) was significantly increased after p-doping process. The peak intensity ratios of each component in the C 1*s* spectra are summarized

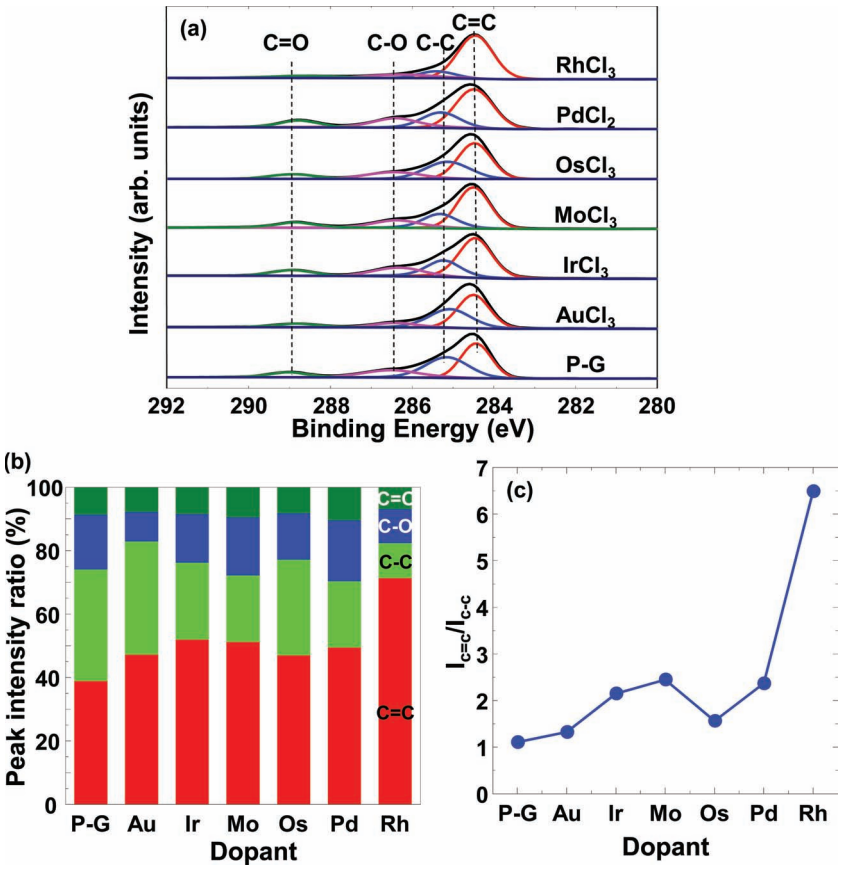


**Figure 5.** a) XPS C 1s spectra of p-doped graphene film: $sp^2$ carbon (C=C) at 284.3 eV, $sp^3$ carbon (C=C) at 285.4 eV, C−O bond at 286.6 eV, and a carbonyl group (C=O) near 288.5 eV were considered. b) Peak intensity ratios of each component in C 1s spectra. c) Ratio of $I_{C=C}$ to $I_{C-C}$. The $I_{C=C}/I_{C-C}$ intensity ratio increased after doping treatment in all samples.

in Figure 5b. The percentage of the C=C bond was significantly increased, but that of the C−C bond was decreased. The largest change of $I_{C=C}$ was found in the case of rhodium. Figure 5c shows the ratio of $I_{C=C}$ to $I_{C-C}$. The $I_{C=C}/I_{C-C}$ intensity ratio increased after doping treatment in all samples. We considered the increase of the $I_{C=C}/I_{C-C}$ intensity ratio to represent further evidence for p-doping by electron transfer from graphene sheets to metal ions.

In order to verify the p-doping of graphene films by metal chloride solutions, the UPS spectra were measured. Figures SI3, SI4, and SI5 show the UPS spectra around the secondary electrons threshold region of the graphene films treated with metal chloride solution of concentrations 5, 10, and 20 mM, respectively. A gold plate is used for correction values. The secondary electron threshold was determined by extrapolating two solid lines from the background and straight onset in the secondary electron threshold region of the UPS spectra.[32] The work function ($\Phi$) is determined from the secondary electron threshold as $\Phi = h\nu - E_{th}$, where $h\nu$ and $E_{th}$ are the photon energy of excitation light (He I discharge lamp, 21.2 eV) and the secondary electron threshold energy, respectively. **Figure 6**a shows the work function variation as a function of each p-dopant with different concentrations. The work function of the PG sample was determined to be about 4.2 eV, which is close to that of graphite. The work function increased with increasing dopant concentration. Figure 6b shows the work function of graphene doped with 20 mM solution. UPS data were taken from different sample positions and the averaged results are shown in Figure 6b. The work function of all samples was greater than that of PG. The work function of $AuCl_3$-doped graphene, a well-known p-dopant material, in our result was similar to that of previous reports.[21–22] Among our six p-dopants, the work function of $RhCl_3$-doped graphene was 5.14 eV, indicating that $RhCl_3$ was the strongest p-dopant.

### 2.4. The Mechanism of p-Doped Graphene Film

Based on these experimental observations, the electron transfer mechanism from graphene to metal ion can be explained as follows. **Figure 7** presents the schematic doping mechanism of graphene by a metal chloride. It has been reported that $AuCl_3$, $IrCl_3$, $MoCl_3$, $OsCl_3$, $PdCl_3$, and $RhCl_3$ have positive reduction potentials, suggesting a great tendency to accept charges from other materials,[32] and the Gibbs free energies obtained from the Nernst equation are −145.7, −179.912, −57.969, −121.336, −125.102, and −156.7 kJ/mol, respectively.[33] These data indicates that metal ions have positive reduction potentials and that the reduction process from $Me^{3+}$ from $Me^0$ is a spontaneous reaction. The expected reaction between metal chloride and graphene is written as follows.[34]

$$\text{Graphene} + 3MeCl_3 \rightarrow \text{Graphene} + MeCl_2^- + Me(I) + MeCl_4^-$$

$$3MeCl_2^- \rightarrow Me^0 + 2MeCl_4^- + 2Cl^-$$

$$MeCl_4^- + \text{Graphene} \rightarrow \text{Graphene}^+ + Me^0 + 4Cl^-$$

According to this reaction, electron transfer occurred from graphene to metal chloride and the resulting depletion of electrons near the Dirac point of PG increased the work function of graphene. The increase of $I_{C=C}/I_{C-C}$ intensity ratio, as shown in Figure 5c, represented further evidence for p-doping by electron transfer from graphene sheets to metal ions. However, it has been observed that sheet resistance of doped graphene slightly increased with keeping time in air, as shown in Figure SI6 (Supporting Information).

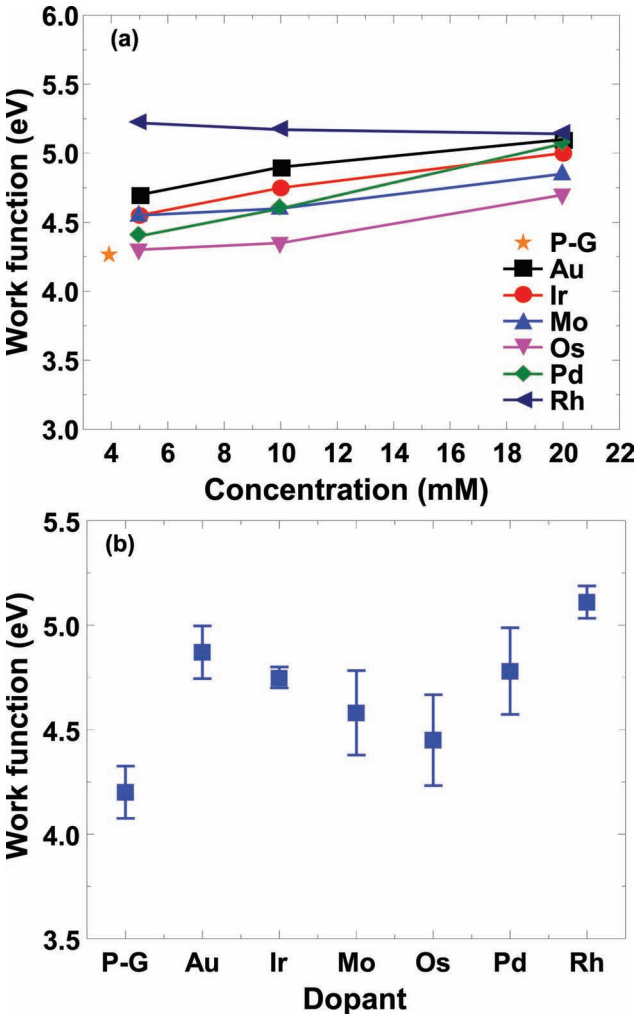


**Figure 6.** a) Work function variation as a function of each p-dopant with different concentrations. The work function increased with increasing dopant concentration. b) Work function of graphene doped with 20 mM solution. UPS data were taken from different sample positions and the results were averaged.

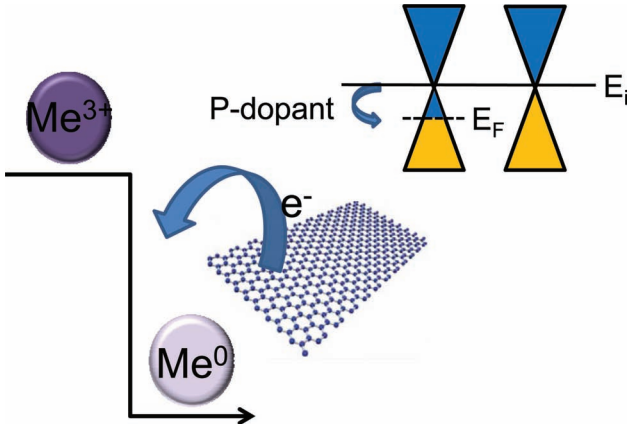


**Figure 7.** Schematic of the mechanism for graphene doping by metal chloride. Metal ions have positive reduction potentials and the reduction process from $Me^{3+}$ to $Me^0$ is a spontaneous reaction. The transfer of electrons from graphene to the metal chloride depleted the electrons near the Dirac point of PG, thereby increasing the work function of graphene.

## 3. Conclusions

The increased work function in graphene achieved by chemical doping using six metal chlorides was investigated. Graphene sheets were synthesized by CVD in optimized condition. The sheet resistance of the doped graphene decreased from 1100 Ω/sq to 500–700 Ω/sq, indicating an increased hole concentration due to charge transfer. However, the transmittance of the doped graphene at 550 nm also decreased from 96.7% to 93% for 20 mM $AuCl_3$ due to the formation of metal particles. The sheet resistance and transmittance were decreased with increasing metal chloride concentration. EDS and XPS data revealed a reduction reaction between the graphene layer and the p-dopant metal ions, leading to the formation of metal particles on the surface. The G peak in the Raman spectra was shifted to a higher wavenumber after metal chloride doping, indicative of a charge transfer from graphene to metal ions. The intensity ratio of $I_{C=C}/I_{C-C}$ increased with doping, indicating an electron transfer from graphene sheets to metal ions. According to UPS data, the work function of graphene increased from 4.2 eV to 5.14 eV for the $RhCl_3$-doped graphene, which was the strongest p-dopant. We considered that spontaneous charge transfer occurred from the specific energy level of graphene to the metal ions, thus increasing the work function. Therefore, the metal chlorides increased the hole concentration at the pristine graphene surface by charge transfer, thus increasing the work function and decreasing the sheet resistance.

## 4. Experimental Section

*Preparation of Graphene*: Few-layer graphene samples were grown on 25-μm-thick copper foil in a quartz tube furnace system using chemical vapor deposition (CVD) involving methane ($CH_4$) and hydrogen ($H_2$) gas. Under vacuum condtions of 90 mTorr, the furnace was heated without any gas flow for 30 min. Before the graphene growth, copper foil was preheated at 950 °C for 30 min. In order to obtain a large, single-crystal copper surface, hydrogen gas at 35 sccm flowed in the furnace under 150 mTorr. After the preheating step, a gas mixture of $CH_4$:$H_2$ = 100 sccm:35 sccm flowed at ambient condition for 10 min to synthesize of graphene. After 10 min of growth, the furnace was cooled quickly to room temperature under 35 sccm hydrogen flow.

*Transfer of Graphene*: After graphene growth, poly[methyl methacrylate] (PMMA, 46 mg/mL in chlorobenzene) was spin-coated on the graphene-coated coated copper foil, which was then baked at 180 °C for 1 min. Then, $O_2$ plasma was used to etch the graphene on the other side of the copper foil. The sample was then immersed in a ferric chloride (1 M $FeCl_3$) bath at room temperature for at least 12 h to etch away the copper foil. After etching, the remaining PMMA-coated graphene on the copper foil was carefully dipped into a deionized water bath more than 7 times to remove any residual etchant. Then, the PMMA-coated graphene sheets were transferred onto an arbitrary substrate. PMMA was removed by immersion in an acetone bath at 80 °C for 30 min after the PMMA/graphene layer had completely adhered onto the target substrate.

*Doping of Transferred Graphene*: Six metal chloride powders, namely, $AuCl_3$, $MoCl_3$, $OsCl_3$, $IrCl_3$, $PdCl_2$, and $RhCl_3$, with high work function were prepared. The each metal chloride powder was dissolved in nitromethane ($AuCl_3$), tetrahydrofuran ($MoCl_3$), acetonitrile ($OsCl_3$, $IrCl_3$), diethyl ether ($PdCl_2$), and methyl alcohol ($RhCl_3$) at a concentration of 5 mM, 10 mM, and 20 mM. After the metal chloride powder had been dissolved in each solvent, the doping solution with three different concentrations was spin-coated (2500 rpm, 1 min, 300 μL) on the transferred graphene substrates.

*Characterization of Graphene and Doped Graphene Films*: Optical micrographs (OM) were acquired by a digital camera (Lumix DMC-LX5, Panasonic). UV-visible spectra were recorded out on a JASCO V-740

photospectrometer with wavelength range from 400 nm to 900 nm. Field emission scanning electron microscopy (FE-SEM; JEOL, JSM-5410LV, Japan) images of the pristine and doped graphene films were also obtained. Raman spectroscopy spectra of graphene were obtained with LabRAM HR (Horiba Jobin Yvon) at an excitation wavelength of 514.54 nm. X-ray photoemission spectroscopy (XPS) was conducted on a Sigma Probe model (ThermoVG, U.K) operating at a base pressure of $5 \times 10^{-10}$ mbar at 300 K with a nonmonochromatized Al K$\alpha$ line at 1486.6 eV, a spherical sector analyzer of 180°, a mean diameter of 275 mm, an analysis area of 15 µm to 400 µm, and multichannel detectors. The results were corrected for charging effects by using C 1s as an internal reference and the Fermi edge of a gold sample. Ultraviolet photoemission spectroscopy (UPS) was performed by on a PHI 5000 VersaProbe with an He I (21.2eV) source.

## Supporting Information

Supporting Information is available from the Wiley Online Library or from the author.

## Acknowledgements

This research was supported in part by Basic Science Research Program (2011-0008994) and Mid-career Research Program (2011-0028752) through the National Research Foundation of Korea (NRF) funded by the Ministry of Education Science and Technology and in part by the Chung-Ang University excellent freshman scholarship grants.

Received: April 9, 2012
Revised: June 16, 2012
Published online: July 5, 2012

[1] A. K. Geim, *Science* **2009**, *324*, 1530.
[2] A. K. Geim, K. S. Novoselov, *Nat. Mater.* **2007**, *6*, 183.
[3] X. Du, I. Skachko, A. Barker, E. Y. Anderi, *Nat. Nanotechnol.* **2008**, *3*, 491.
[4] K. S. Novoselov, Z. Jiang, Y. Zhang, S. V. Morozov, H. L. Stormer, U. Zeitler, J. C. Maan, G. S. Boebinger, P. Kim, A. K. Geim, *Science* **2007**, *315*, 1379.
[5] Y. Zhnag, Y.-W. Tan, H. L. Stormer, P. Kim, *Nature* **2005**, *438*, 201.
[6] D. Gunlycke, H. M. Lawler, C. T. White, *Phys. Rev. B* **2007**, *75*, 085418.
[7] K. S. Kim, Y. Zhao, H. Jang, S. Y. Lee, J. M. Kim, K. S. Kim, J.-H. Ahn, P. Kim, J.-Y. Choi, B. H. Hong, *Nature* **2009**, *457*, 706.
[8] A. Reina, X. Jia, J. Ho, D Nezich, H. Son, V. Bulovic, M. S. Dresselhaus, J. Kong, *Nano. Lett.* **2009**, *9*, 30.
[9] X. Li, W. Cai, J. An, S. Kim, J. Nah, D. Yang, R. Piner, A. Velamakanni, I. Jung, E. Tutuc, S. K. Banerjee, L. Colombo, R. S. Ruoff, *Science* **2009**, *324*, 1312.
[10] Q. Yu, L. A. Jauregui, W. Wu, R. Colby, J. Tian, Z. Su, H. Cao, Z. Liu, D. Pandey, D. Wei, T. F. Chung, P. Peng, N. P. Guisinger, E. A. Stach, J. Bao, S.-S. Pei, Y. P. Chen, *Nat. Mater.* **2011**, *10*, 444.
[11] J. Sun, M. T. Cole, N. Lindvall, K. B. K. Teo, A. Yurgens, *Appl. Phys. Lett.* **2012**, *100*, 022102.
[12] R. S. Weatherup, B. C. Bayer, R. Blume, C. Ducati, C. Baehtz, R. Schlögl, S. Hofmann, *Nano Lett.* **2011**, *11*, 4154.
[13] S. Bae, H. Kim, Y. Lee, X. Xu, J.-S. Park, Y. Zheng, J. Balakrishnan, T. Lei, H. R. Kim, Y. I. Song, Y.-J. Kim, K. S. Kim, B. Özyilmaz, J.-H. Ahn, B. H. Hong, S. Iijima, *Nat. Nanotechnol.* **2010**, *5*, 574.
[14] T. H. Seo, K. J. Lee, T. S. Oh, Y. S. Lee, H. Jeong, A. H. Park, H. Kim, Y. R. Choi, E.-K. Suh, T. V. Cuong, V. H. Pham, J. S. Chung, E. J. Kim, *Appl. Phys. Lett.* **2011**, *98*, 251114.
[15] G. Jo, M. Choe, C.-Y. Cho, J. H. Kim, W. Park, S. Lee, W.-K. Hong, T.-W. Kim, S.-J. Park, B. H. Hong, Y. H. Kahng, T. Lee, *Nanotechnology* **2010**, *21*, 175201.
[16] T. Sun, Z. L. Wang, Z. J. Shi, G. Z. Ran, W. J. Xu, Z. Y. Wang, Y. Z. Li, L. Dai, G. G. Qin, *Appl. Phys. Lett.* **2010**, *96*, 133301.
[17] T.-H. Han, Y. Lee, M.-R. Choi, S.-H. Woo, S.-H. Bae, B. H. Hong, J.-H. Ahn, T.-W. Lee, *Nat. Photonics* **2012**, *6*, 105.
[18] M. Cox, A. Gorodetsky, B. Kim, K. S. Kim, Z. Jia, P. Kim, C. Nuckolls, I. Kymissis, *Appl. Phys. Lett.* **2011**, *98*, 123303.
[19] M. Choe, B. H. Lee, G. Jo, J. Park, W. Park, S. Lee, W.-K. Hong, M.-J. Seong, Y. H. Kahng, K. Lee, T. Lee, *Org. Electron.* **2010**, *11*, 1864.
[20] S. Pang, Y. Hernandex, X. Feng, K. Müllen, *Adv. Mater.* **2011**, *23*, 2779.
[21] H.-J. Shin, W. M. Choi, D. Choi, G. H. Han, S.-M. Yoon, H.-K. Park, S.-W. Kim, Y. W. Jin, S. Y. Lee, J. M. Kim, J.-Y. Choi, Y. H. Lee, *J. Am. Chem. Soc.* **2010**, *132*, 15603.
[22] A. Benayad, H.-J. Shin, H. K. Park, S.-M. Yoon, K. K. Kim, M. H. Jin, H.-K. Jeong, J. C. Lee, J.-Y. Choi, Y. H. Lee, *Chem. Phys. Lett.* **2009**, *475*, 91.
[23] D. Wei, Y. Liu, Y. Wang, H. Zhang, L. Huang, G. Yu, *Nano. Lett.* **2009**, *9*, 1752.
[24] Y. Shi, K. K. Kim, A. Reina, M. Hofmann, L.-J. Li, J. Kong, *ACS Nano* **2010**, *4*, 2689.
[25] J. Park, W. H. Lee, S. Huh, S. H. Sim, S. B. Kim, K. Cho, B. H. Hong, K. S. Kim, *J. Phys. Chem. Lett.* **2011**, *2*, 841.
[26] Y. Wang. S. W. Tong, X. F. Xu, B. Özyilmaz, K. P. Loh, *Adv. Mater.* **2011**, *23*, 1514.
[27] D. R. Lide, *CRC handbook on Chemistry and Physics*, CRC Press LLC, Cleveland, OH **2008**, p.12–114.
[28] S. Pisana, M. Lazzeri, C. Casiraghi, K. S. Novoselov, A. K. Geim, A. C. Ferrari, F. Mauri, *Nat. Mater.* **2007**, *6*, 198.
[29] A. Das, S. Pisana, B. Chakraborty, S. Piscanec, S. K. Saha, U. V. Waghmare, K. S. Novoselov, H. R. Krishnamurthy, A. K. Geim, A. C. Ferrari, A. K. Sood, *Nat. Nanotechnol.* **2008**, *3*, 210.
[30] S. Y. Kim, K. Hong, J.-L. Lee, *Jpn. J. Appl. Phys.* **2011**, *50*, 101602.
[31] Y. U. Ko, S.-R. Cho, K. S. Choi, Y. Park, S. T. Kim, N. H. Kim, S. Y. Kim, S. T. Chang, *J. Mater. Chem.* **2012**, *22*, 3606.
[32] S. Y. Kim, K. Hong, K. Kim, H. K. Yu, W-K. Kim, J. L. Lee, *J. Appl. Phys.* **2008**, *103*, 076101.
[33] J. A. Dean, *Lange's Handbook of Chemistry*, 12th ed., McGraw-Hill Book Company, New York **1979**, p. 9:4–9:94.
[34] S. M. Kim, K. K. Kim, Y. W. Jo, M. H. Park, S. J. Chae, D. L. Duong, C. W. Yang, J. Kong, Y. H. Lee, *ACS Nano* **2011**, *5*, 1236.